

Electronic supplemental information for

**Consequences of changes in ZnO trap distribution on the performance
of dye-sensitized solar cells**

J. Falgenhauer, F. Fiehler, C. Richter, M. Rudolph and D. Schlettwein

Institute of Applied Physics, Justus-Liebig-University, Heinrich-Buff-Ring 16,
35392 Giessen, Germany. E-mail: schlettwein@uni-giessen.de;
Fax: +49 641 99 33409; Tel: +49 641 99 33401

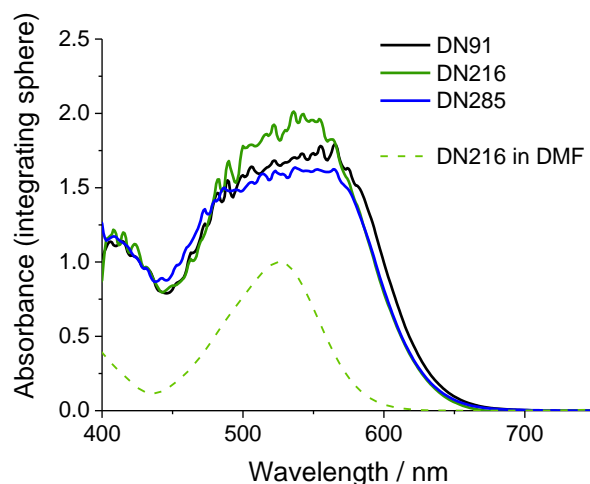


Fig. S1 Absorbance measurements of films sensitized according to the sensitization procedures described in the main article with dyes DN91, DN216 and DN285, and a coadsorbate. The absorbance of a dilute solution of the dye DN216 in dimethylformamide is represented by a dashed line (maximum normalized to 1). Very similar absorbance in solution is found for other indoline dyes discussed in this work ¹.

In Figure S1 absorbance spectra are shown of sensitized porous ZnO films equivalent to those used for the cells discussed in the main article. The absorbance spectra of the dyes DN91, DN216 and DN285 adsorbed to the ZnO electrodes show almost identical characteristics, indicating, further, a dye loading appropriate for DSSC in all cases as clearly proven by similarity to the spectrum in solution and by the slope above 580 nm despite scattering of data below 580 nm. As the films were highly scattering, an integrating sphere setup was used for the absorbance measurements, thus detecting also forward scattered light. Signals by the FTO/glass substrate and the ZnO films were subtracted from the overall signal to yield the best estimate of the absorbance caused by the adsorbed dye. The broadened spectrum, compared to the absorbance of a dilute solution of DN216, indicates close proximity of the dye molecules ² as a direct consequence of a high dye loading. Comparable films sensitized with D149 of similar absorbance were shown ^{3,4} to have a dye loading of about $9 \cdot 10^{-5} \text{ mol cm}^{-3}$. With an inner surface area ⁵ of more than $5 \cdot 10^5 \text{ cm}^2 \text{ cm}^{-3}$, and a size of the dye molecules of several Å, the ZnO surface should thus be well covered with adsorbed molecules. Such high dye loading led to strong light absorption needed for well-functioning DSSCs, but exceeding the detection limit of the spectrometer, thus causing the noise in the acquired transmission spectra of Figure S1.

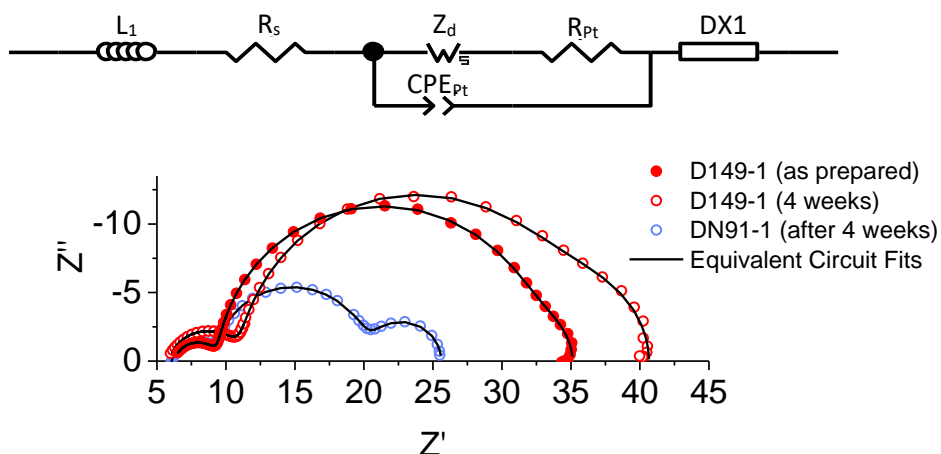


Fig. S2 (a) Equivalent circuit used for the fitting of electrochemical impedance spectroscopy (EIS) data with the elements L_1 (inductance of contacts and wires), R_s (series resistance of substrate), Z_d (Warburg element, representing electrolyte diffusion), CPE_{Pt} and R_{Pt} (charge transfer at the platinized counter electrode, with constant phase element and resistance, respectively), $DX1$ (distributed element, describing charge transfer at the active layer). (b) Measured EIS spectra at a voltage of -0.60 V (symbols) and fitting according to the equivalent circuit in (a) (black lines).

Electrochemical impedance spectra were evaluated by fitting with the equivalent circuit shown in Fig. S2(a) using the program *ZView*. The equivalent circuit represents an established scheme (see for example ^{6,7}), with slight modifications to account for contacts and wiring. Results for three measured spectra are shown in Fig. S2(b). The values obtained from such fits are used to determine R_s , C_μ and R_{rec} discussed in the main text. Since $DX1$ is a distributed element representing a transmission line (see ^{8,9} and ¹⁰ with cited references), internally listed parameters ($DX1-C$ and $DX1-D$ with its exponent $DX1-E$) in *ZView* have to be used for R_{rec} and C_μ , respectively, using $C_\mu = (DX1-D)^{(1/DX1-E)}$ to account for the constant phase character of the element.

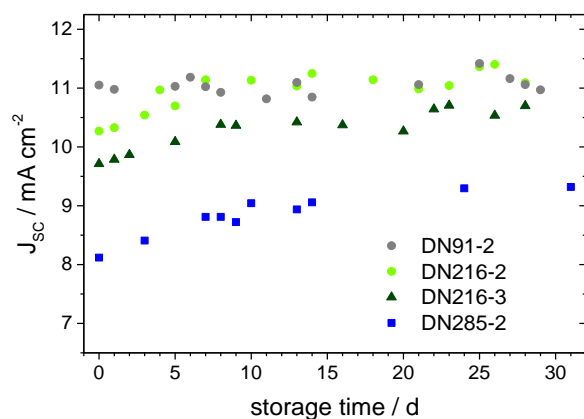


Fig. S3 As in Fig. 3 of the main text for cells not included there.

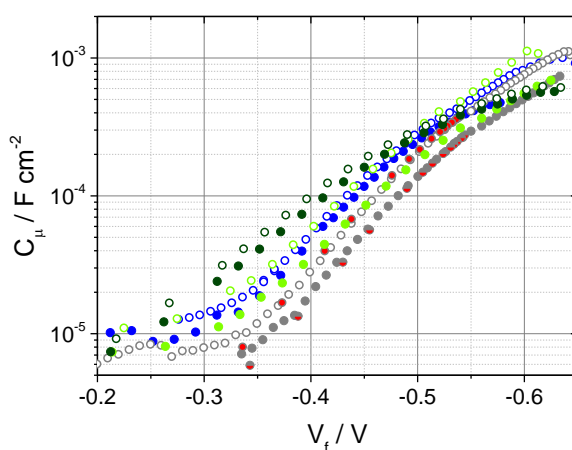


Fig. S4 As in Fig. 4 of the main text for cells not included there. Cell DN91 (2) was additionally characterized by EIS at red LED illumination, indicated by grey circles half-filled in red (after preparation) and filled (after storage in the dark).

A shift of C_μ to less negative potentials as observed in Fig. 4 (main article) and Fig. S4 is assigned to a change in energy levels at the dye-semiconductor interface (see discussion in main text following Table 2), which is supported by an accompanying increase of the current density. It could, however, also be caused by a shift of the electrolyte redox potential to higher energies since the voltage is referenced to this value. If regeneration of the dye is limited under AM1.5 illumination in the cells directly after preparation, an increase of the current density after storage could also be achieved by a shift of the redox level and, thus, an increase in the driving force for regeneration. In an independent experiment (not shown here) cells were, therefore, filled with an electrolyte aged in contact to air and no difference in the chemical capacitance compared to a cell with freshly prepared electrolyte was observed. A possible influence of aged electrolyte was thereby excluded and the observed shift in C_μ was safely traced back to changes at the ZnO surface.

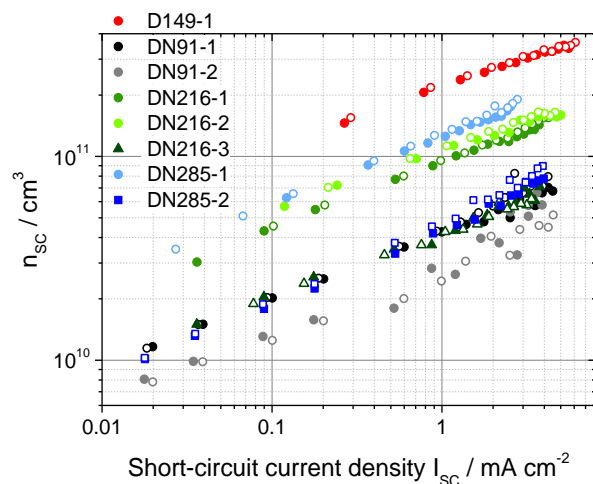


Fig. S5 Electron density at short circuit n_{SC} , determined from short-circuit current density transient measurements of indoline-based DSSCs. Filled symbols indicate measurements after preparation, open symbols indicate measurements performed after 4 weeks storage of the cells in the dark. The different colors indicate different cells and sensitizers according to the legend.

Charge extraction measurements (photocurrent transients) were performed at red LED illumination with varying illumination intensity. The charge at short circuit, Q_{SC} , was determined by an integration of the curve after turning the light off. Q_{SC} was used to calculate ¹¹ the short-circuit charge density n_{SC} (Fig. S5) after $n_{SC} = Q_{SC}/(qAd[1 - p])$, with q the elemental charge, A the projected area of the solar cell active layer, d the thickness of the film and p the porosity of the film (assumed to be 0.6 ¹¹). The curves were normalized by use of the relative total trap density $N_t/N_{t,ref}$ ¹¹ (Table 2, main article) to overlap with the curve of cell D149-1 (directly after preparation).

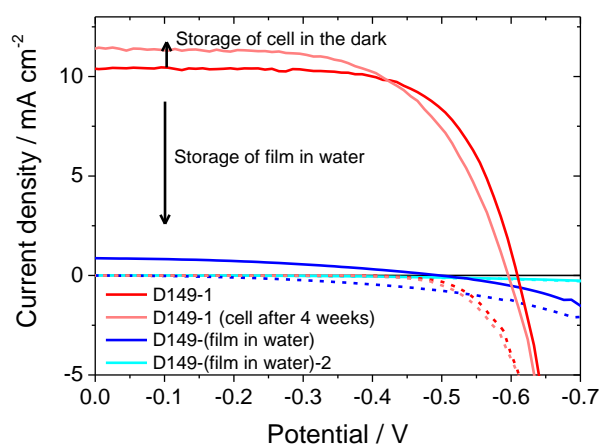


Fig. S6 *IV*-curves of two cells prepared from ZnO films stored in water for more than 100 days (blue and cyan curves), and a reference cell D149 (directly after preparation of the cell – darker red curve – and after storage of the cell in the dark for 4 weeks – lighter red curve). *IV*-curves measured in the dark are indicated by dashed lines, while *IV*-curves measured at simulated AM1.5 illumination are indicated by solid lines.

In additional experiments, films were stored in distilled water for more than 100 days following the desorption of the structure directing agents. Subsequently, cells were prepared as described in the main article, starting with a sensitization of the dried ZnO film with D149 and lithocholic acid. The sensitized films showed an intense coloring similar to the reference cell D149-1. Current-voltage curves (*IV*-curves) of two completed cells, cells D149-(film in water) and D149-(film in water)-2, are shown in Fig. S6. While a storage of regular cells in the dark leads to an increase of J_{sc} (see main text), J_{sc} is much lower for the cells based on films stored in water, as is the power-conversion efficiency, see also Table S2. The recombination current density at more negative voltages is also reduced for these cells, pointing at a favorably increased R_{rec} .

Table S2 Cell parameters for ZnO dye-sensitized solar cells where the films were stored in water before film preparation, and a reference cell, D149, which was measured directly after preparation, and after a storage in the dark for 4 weeks. The measurement type “direct” indicates the measurement directly after cell preparation.

Cell	measurement	J_{sc} / mA cm ⁻² at AM1.5	V_{oc} / V	FF	η / %
D149-(film in water)	direct	0.8679	-0.497	0.39	0.17
D149-(film in water)-2	direct	0.0028	-0.122	0.35	0.00
D149	direct	10.38	-0.609	0.68	4.29
	after 4 weeks	11.45	-0.596	0.62	4.15

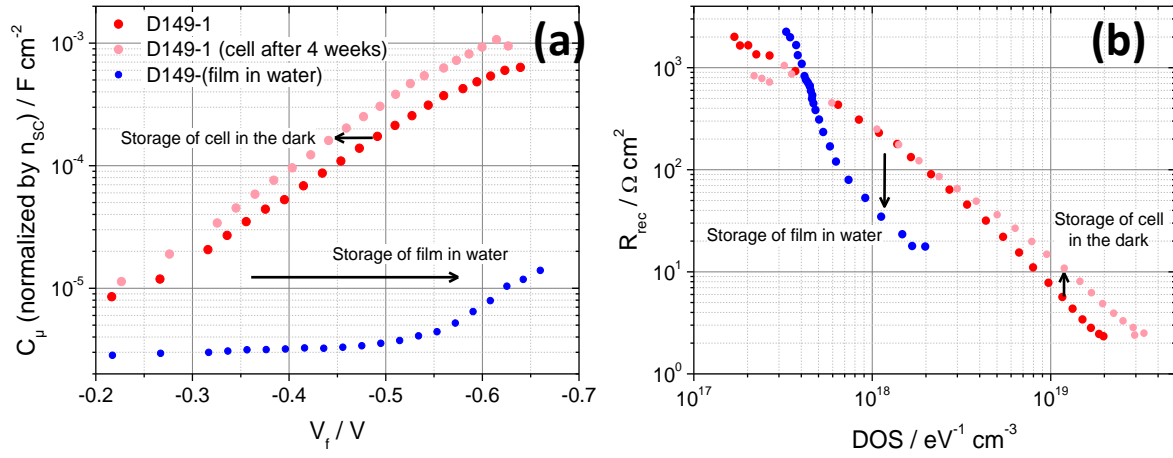


Fig. S7 Chemical capacitance of a cell prepared from ZnO films stored in water for more than 100 days (blue symbols), and a reference cell D149 (directly after preparation of the cell – darker red curve – and after storage of the cell in the dark for 4 weeks – lighter red curve).

For the cell D149-(film in water) the chemical capacitance C_μ was determined from electrochemical impedance spectroscopy measurements, and is shown in Fig. S7 (with normalization by the relative total trap density $N_V/N_{t,ref}$ for the evaluation of the shift of the conduction band edge¹¹). This measurement is compared with a reference cell D149, measured directly after preparation of the cell and after a storage of the cell in the dark for 4 weeks. Compared to the reference cell D149 measured directly after preparation, a storage of the unsensitized **film** in water leads to a shift of E_c to higher energies by almost 300 mV, indicating a strong decrease of the density of states at a given energy. The storage of the reference **cell** in the dark on the other hand leads to a shift of E_c to lower energies by about 40 mV (see main text). The observed decrease of the density of states at a certain energy for, e.g., cell D149 (film in water) provides an explanation of the low J_{SC} , as a higher E_c leads to a lower injection efficiency¹². However, such lower density of states offers less opportunity for recombination, which then leads to the lower recombination current observed in the IV -curves of cells D149-(film in water) and D149-(film in water)-2 in Fig. S6.

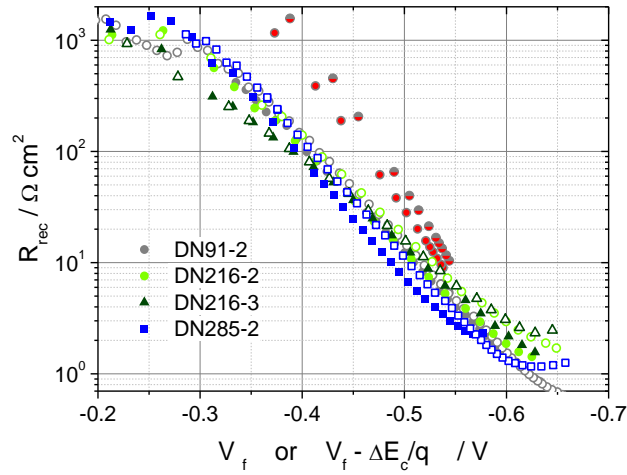


Fig. S8 As in Fig. 5 of the main text for cells not included there. Cell DN91 (2) was additionally characterized by EIS at red LED illumination, indicated by grey circles half-filled in red (after preparation) and filled (after storage in the dark).

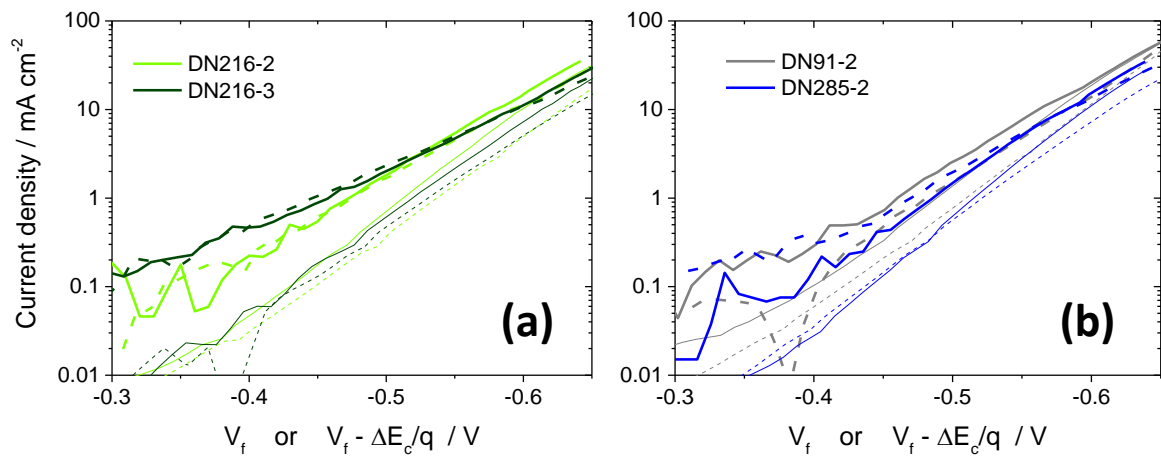


Fig. S9 As in Fig. 6 of the main text for cells not included there. Sensitization with (a) dye DN216 and (b) dyes DN91 or DN285.

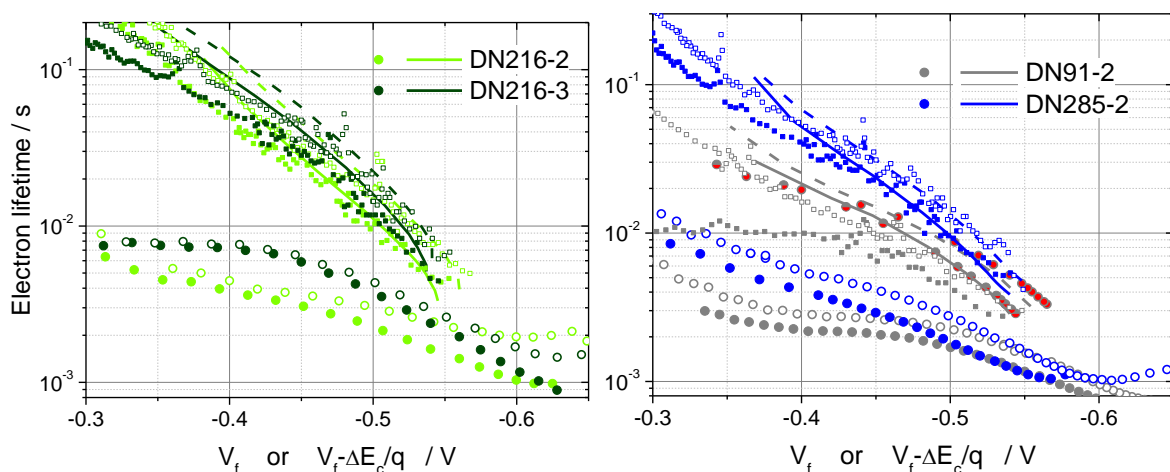


Fig. S10 As in Fig. 7 of the main text for cells not included there. Cell DN91 (2) was additionally characterized by EIS at red LED illumination, indicated by grey circles half-filled in red (after preparation) and filled (after storage in the dark).

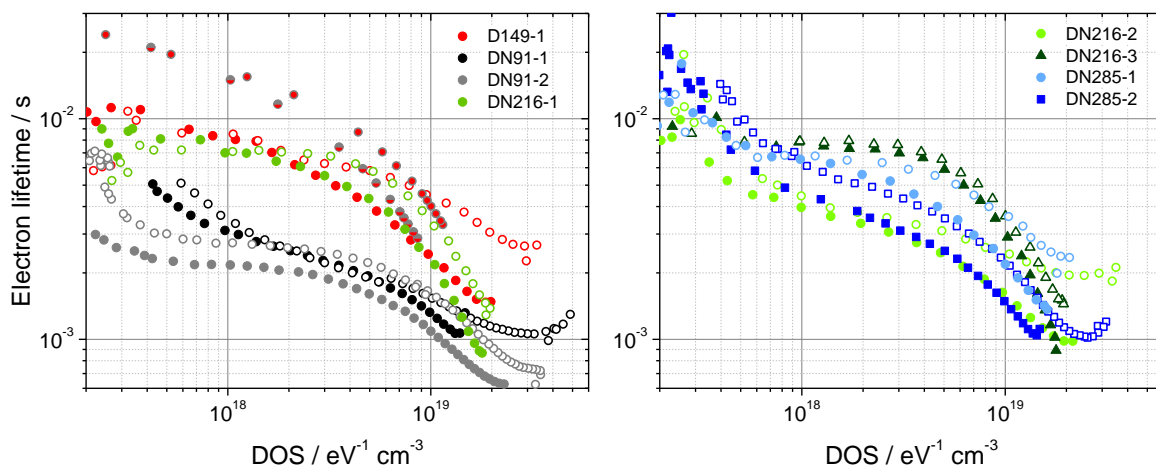


Fig. S11 Electron lifetime vs. DOS. Filled symbols indicate measurements directly after preparation of the cells, open symbols indicate measurements after 4 weeks storage in the dark for 4 weeks. Different colors indicate different sensitizers or cells according to the legend. Cell DN91 (2) was additionally characterized by EIS at red LED illumination, indicated by grey circles half-filled (after preparation) and filled (after storage in the dark) with red.

A plot of the electron lifetime against the density of states (DOS) allows a comparison of the recombination of the different cells (Fig. S11), as contributions of different trap distributions on recombination due to different DOS are eliminated. In tendency, the sensitized DN91 seems to lead to an overall lower electron lifetime than the other indoline sensitizers, which indicates that recombination is slightly enhanced for electrodes sensitized with DN91 compared to DN216, DN285 or D149.

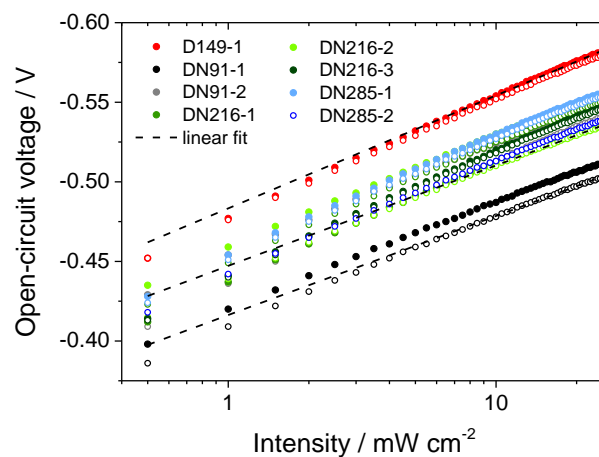


Fig. S12 Open-circuit voltage measured vs. illumination intensity (red LED illumination) for indoline-sensitized DSSCs before and after storage in the dark for 4 weeks. Filled symbols indicate measurements directly after cell preparation, and open symbols indicate measurements after storage in the dark for 4 weeks (for cell DN285-2 only measurement after 4 weeks available). Different indoline dyes and different cells are indicated by different colors, see the legend for exact designation. Linear fits (fitted to the values at higher intensities) are shown for three representative measurements.

Measurements of V_{OC} at different illumination intensities were performed, and the measurements for cells consisting of ZnO electrodes sensitized by different indoline dyes are shown in Fig. S12. The recombination parameter β was determined from the inverse slope of the curves⁶ at higher light intensities (fit indicated in the plot for some of the cells), see Table 2 in the main text for the values of β .

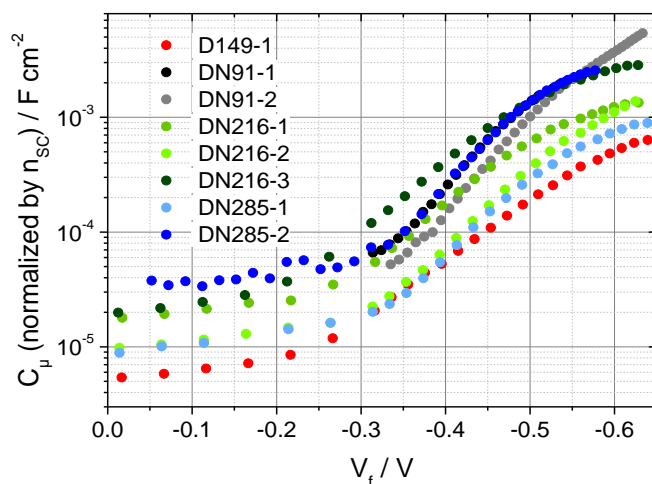


Fig. S13 Chemical capacitance C_μ corrected by the value of the relative total trap density $N_t/N_{t,ref}$. Only measurements directly after preparation are shown, due to the similarity of n_{sc} before and after ageing. Different colors indicate different sensitizers and cells, according to the legend.

C_μ was corrected by $N_t/N_{t,ref}$ ¹¹ (determined from n_{sc}) to determine relative shifts of E_C for the different cells, see Fig. S13. This correction is not needed for the comparison of the measurements directly after preparation with the measurements after ageing of cells, but for a direct comparison of individual cells. The cells do not show identical E_C , and no clear dependence on the sensitizing dye. The random distribution of E_C and, thereby, of the voltage-dependence of the C_μ -curve is probably due to small differences in processing during the electrochemical deposition of the films or slight compositional differences across the substrate material (fluorine-doped tin oxide-coated glass) and, consequently, differences in the trap distribution in the ZnO films used for the different cells.

References

- ¹ Falgenhauer, J.; Richter, C.; Miura, H.; Schlettwein, D. Stable Sensitization of ZnO by Improved Anchoring of Indoline Dyes. *ChemPhysChem* **2012**, *13* (12), 2893–2897. DOI: 10.1002/cphc.201200085.
- ² Fakis, M.; Stathatos, E.; Tsigaridas, G.; Giannetas, V.; Persephonis, P. Femtosecond Decay and Electron Transfer Dynamics of the Organic Sensitizer D149 and Photovoltaic Performance in Quasi-Solid-State Dye-Sensitized Solar Cells. *J. Phys. Chem. C* **2011**, *115* (27), 13429–13437. DOI: 10.1021/jp201143n.
- ³ Magne, C.; Moehl, T.; Urien, M.; Grätzel, M.; Pauporté, T. Effects of ZnO film growth route and nanostructure on electron transport and recombination in dye-sensitized solar cells. *J. Mater. Chem. A* **2013**, *1* (6), 2079–2088. DOI: 10.1039/c2ta00674j.
- ⁴ Tefashe, U. M.; Rudolph, M.; Miura, H.; Schlettwein, D.; Wittstock, G. Photovoltaic characteristics and dye regeneration kinetics in D149-sensitized ZnO with varied dye loading and film thickness. *Phys. Chem. Chem. Phys.*, **2012**, *14*, 7533–7542. DOI: 10.1039/C2CP40798A.
- ⁵ Pauporte, T.; Rathousky, J. Electrodeposited Mesoporous ZnO Thin Films as Efficient Photocatalysts for the Degradation of Dye Pollutants. *J. Phys. Chem. C* **2007**, *111* (21), 7639–7644. DOI: 10.1021/jp071465f.

-
- ⁶ Guillén, E.; Peter, L. M.; Anta, J. A. Electron Transport and Recombination in ZnO-Based Dye-Sensitized Solar Cells. *J. Phys. Chem. C* **2011**, *115* (45), 22622–22632. DOI: 10.1021/jp206698t.
- ⁷ Rudolph, M.; Yoshida, T.; Schlettwein, D. Influence of indoline dye and coadsorbate molecules on photovoltaic performance and recombination in dye-sensitized solar cells based on electrodeposited ZnO. *J. Electroanal. Chem.* **2013**, *709*, 10–18. DOI: 10.1016/j.jelechem.2013.09.028.
- ⁸ Bisquert, J.; Garcia-Belmonte, G.; Fabregat-Santiago, F.; Compte, A. Anomalous transport effects in the impedance of porous film electrodes. *Electrochemistry Communications* **1999**, *1* (9), 429–435. DOI: 10.1016/S1388-2481(99)00084-3.
- ⁹ Bisquert, J. Influence of the boundaries in the impedance of porous film electrodes. *Phys. Chem. Chem. Phys.* **2000**, *2* (18), 4185–4192. DOI: 10.1039/b001708f.
- ¹⁰ Fabregat-Santiago, F.; Garcia-Belmonte, G.; Mora-Seró, I.; Bisquert, J. Characterization of nanostructured hybrid and organic solar cells by impedance spectroscopy. *Phys. Chem. Chem. Phys.* **2011**, *13* (20), 9083–9118. DOI: 10.1039/c0cp02249g.
- ¹¹ Rudolph, M.; Yoshida, T.; Miura, H.; Schlettwein, D. Improvement of Light Harvesting by Addition of a Long-Wavelength Absorber in Dye-Sensitized Solar Cells Based on ZnO and Indoline Dyes. *J. Phys. Chem. C* **2015**, *119* (3), 1298–1311. DOI: 10.1021/jp511122u.
- ¹² Hagfeldt, A.; Boschloo, G.; Sun, L.; Kloo, L.; Pettersson, H. Dye-Sensitized Solar Cells. *Chem. Rev.* **2010**, *110* (11), 6595–6663. DOI: 10.1021/cr900356p.